High-modulation efficiency operation of GaInAsP/InP membrane distributed feedback laser on Si substrate

Daisuke Inoue,[1,*] Takuo Hiratani,[1] Kai Fukuda,[1] Takahiro Tomiyasu,[1] Tomohiro Amemiya,[2] Nobuhiko Nishiyama,[1] and Shigehisa Arai[1,2]

[1]*Department of Electrical and Electronic Engineering, Tokyo Institute of Technology, 2-12-1-S9-5 O-okayama, Meguro-ku, Tokyo 152-8552, Japan*

[2]*Quantum Nanoelectronics Research Center, Tokyo Institute of Technology, 2-12-1-S9-5 O-okayama, Meguro-ku, Tokyo 152-8552, Japan*

[*]*inoue.d.ac@m.titech.ac.jp*

Abstract: The direct modulation characteristics of a membrane distributed feedback (DFB) laser on a silicon substrate were investigated. Enhancement of the optical confinement factor in the membrane structure facilitates the fabrication of a strongly index-coupled (κ_i = 1500 cm^{-1}) DFB laser with the cavity length of 80 μm and a threshold current of 270 μA. Small-signal modulation measurements yielded a −3dB bandwidth of 9.5 GHz at 1.03-mA bias current, with modulation efficiency of 9.9 GHz/mA$^{1/2}$, which is, to the best of our knowledge, the highest value among those reported for DFB lasers.

OCIS codes: (230.0230) Optical devices; (140.3490) Lasers, distributed-feedback; (200.4650) Optical interconnects; (250.5960) Semiconductor lasers.

References and links

1. A. Benner, "Optical interconnect opportunities in supercomputers and high end computing," in Optical Fiber Communication Conference (OFC), 2012 OSA Technical Digest Series (Optical Society of America, 2012), paper OTu2B.
2. D. A. B. Miller, "Device requirements for optical interconnects to silicon chips," Proc. IEEE **97**(7), 1166–1185 (2009).
3. S. Imai, K. Takaki, S. Kamiya, H. Shimizu, J. Yoshida, Y. Kawakita, T. Takagi, K. Hiraiwa, H. Shimizu, T. Suzuki, N. Iwai, T. Ishikawa, N. Tsukiji, and A. Kasukawa, "Recorded low power dissipation in highly reliable 1060-nm VCSELs for "Green" optical interconnection," IEEE J. Sel. Top. Quantum Electron. **17**(6), 1614–1620 (2011).
4. P. Moser, J. A. Lott, P. Wolf, G. Larisch, H. Li, N. N. Ledentsov, and D. Bimberg, "56 fJ dissipated energy per bit of oxide-confined 850 nm VCSELs operating at 25 Gbit/s," Electron. Lett. **48**(20), 1292–1294 (2012).
5. C. C. Chang, P. K. Shen, C. T. Chen, H. L. Hsiao, H. C. Lan, Y. C. Lee, and M. L. Wu, "SOI-based trapezoidal waveguide with 45° microreflector for noncoplanar optical interconnect," Opt. Lett. **37**(5), 782–784 (2012).
6. L. Liu, J. Van Campenhout, G. Roelkens, R. A. Soref, D. Van Thourhout, P. Rojo-Romeo, P. Regreny, C. Seassal, J.-M. Fédéli, and R. Baets, "Carrier-injection-based electro-optic modulator on silicon-on-insulator with a heterogeneously integrated III-V microdisk cavity," Opt. Lett. **33**(21), 2518–2520 (2008).
7. J. Lloret, R. Kumar, S. Sales, F. Ramos, G. Morthier, P. Mechet, T. Spuesens, D. Van Thourhout, N. Olivier, J. M. Fédéli, and J. Capmany, "Ultracompact electro-optic phase modulator based on III-V-on-silicon microdisk resonator," Opt. Lett. **37**(12), 2379–2381 (2012).
8. J. Van Campenhout, P. Rojo Romeo, P. Regreny, C. Seassal, D. Van Thourhout, S. Verstuyft, L. Di Cioccio, J.-M. Fedeli, C. Lagahe, and R. Baets, "Electrically pumped InP-based microdisk lasers integrated with a nanophotonic silicon-on-insulator waveguide circuit," Opt. Express **15**(11), 6744–6749 (2007).
9. B. Ellis, M. A. Mayer, G. Shambat, T. Sarmiento, J. Harris, E. E. Haller, and J. Vuckovic, "Ultralow-threshold electrically pumped quantum dot photonic-crystal nanocavity laser," Nat. Photonics **5**(5), 297–300 (2011).
10. K. Takeda, T. Sato, A. Shinya, K. Nozaki, W. Kobayashi, H. Taniyama, M. Notomi, K. Hasebe, T. Kakitsuka, and S. Matsuo, "Few-fJ/bit data transmissions using directly modulated lambda-scale embedded active region photonic-crystal lasers," Nat. Photonics **7**(7), 569–575 (2013).
11. R. S. Tucker, J. M. Wiesenfeld, P. M. Downey, and J. E. Bowers, "Propagation delays and transition times in pulse-modulated semiconductor lasers," Appl. Phys. Lett. **48**(25), 1707–1709 (1986).

#250395 Received 22 Sep 2015; revised 22 Oct 2015; accepted 25 Oct 2015; published 29 Oct 2015

12. S. Arai, N. Nishiyama, T. Maruyama, and T. Okumura, "GaInAsP/InP membrane lasers for optical interconnects," IEEE J. Sel. Top. Quantum Electron. **17**(5), 1381–1389 (2011).
13. K. Oe, Y. Noguchi, and C. Caneau, "GaInAsP lateral current injection lasers on semi-insulating substrates," IEEE Photonics Technol. Lett. **6**(4), 479–481 (1994).
14. T. Okumura, M. Kurokawa, M. Shirao, D. Kondo, H. Ito, N. Nishiyama, T. Maruyama, and S. Arai, "Lateral current injection GaInAsP/InP laser on semi-insulating substrate for membrane-based photonic circuits," Opt. Express **17**(15), 12564–12570 (2009).
15. T. Okamoto, N. Nunoya, Y. Onodera, S. Tamura, and S. Arai, "Continuous wave operation of optically pumped membrane DFB laser," Electron. Lett. **37**(24), 1455–1457 (2001).
16. T. Okamoto, N. Nunoya, Y. Onodera, T. Yamazaki, S. Tamura, and S. Arai, "Optically pumped membrane BH-DFB lasers for low-threshold and single-mode operation," IEEE J. Sel. Top. Quantum Electron. **9**(5), 1361–1366 (2003).
17. S. Sakamoto, H. Naitoh, M. Ohtake, Y. Nishimoto, S. Tamura, T. Maruyama, N. Nishiyama, and S. Arai, "Strongly index-coupled membrane BH-DFB lasers with surface corrugation grating," IEEE J. Sel. Top. Quantum Electron. **13**(5), 1135–1141 (2007).
18. U. D. Dave, B. Kuyken, F. Leo, S.-P. Gorza, S. Combrie, A. De Rossi, F. Raineri, and G. Roelkens, "Nonlinear properties of dispersion engineered InGaP photonic wire waveguides in the telecommunication wavelength range," Opt. Express **23**(4), 4650–4657 (2015).
19. A. Higuera-Rodriguez, V. Dolores-Calzadilla, Y. Jiao, E. J. Geluk, D. Heiss, and M. K. Smit, "Realization of efficient metal grating couplers for membrane-based integrated photonics," Opt. Lett. **40**(12), 2755–2757 (2015).
20. D. Inoue, J. Lee, T. Hiratani, Y. Atsuji, T. Amemiya, N. Nishiyama, and S. Arai, "Sub-milliampere threshold operation of butt-jointed built-in membrane DFB laser bonded on Si substrate," Opt. Express **23**(6), 7771–7778 (2015).
21. D. Inoue, T. Hiratani, Y. Atsuji, T. Tomiyasu, T. Amemiya, N. Nishiyama, and S. Arai, "Monolithic integration of membrane-based butt-jointed built-in DFB lasers and p-i-n photodiodes bonded on Si substrate," IEEE J. Sel. Top. Quantum Electron. **21**(6), 1502907 (2015).
22. T. Hiratani, D. Inoue, T. Tomiyasu, Y. Atsudi, K. Fukuda, T. Amemiya, N. Nishiyama, and S. Arai, "Semiconductor membrane distributed-reflector (DR) laser," in Proceedings of the International Conference on Indium Phosphide and Related Materials (IPRM'2015), Santa Barbara, CA (2015), paper We1O6.1.
23. D. Inoue, J. Lee, K. Doi, T. Hiratani, Y. Atsuji, T. Amemiya, N. Nishiyama, and S. Arai, "Room-temperature continuous-wave operation of GaInAsP/InP lateral-current-injection membrane laser bonded on Si substrate," Appl. Phys. Express **7**(7), 072701 (2014).
24. K. Ohira, T. Murayama, S. Tamura, and S. Arai, "Low-threshold and high-efficiency operation of distributed reflector lasers with width-modulated wirelike active regions," IEEE J. Sel. Top. Quantum Electron. **11**(5), 1162–1168 (2005).
25. S. Matsuo, T. Fujii, K. Hasebe, K. Takeda, T. Sato, and T. Kakitsuka, "Directly modulated DFB laser on SiO_2/Si substrate for datacenter networks," Lightwave Technol. **33**(6), 1217–1222 (2015).
26. S. Kanazawa, T. Ito, T. Sato, R. Iga, W. Kobayashi, K. Takahata, H. Sanjoh, and H. Ishii, "Flip-chip mounted 25.8-Gb/s directly modulated InGaAsP DFB laser with Ru-doped semi-insulating buried heterostructure," IEICE Electron. Express **12**(1), 20141028 (2015).
27. W. Kobayashi, T. Ito, T. Yamanaka, T. Fujisawa, Y. Shibata, T. Kurosaki, M. Kohtoku, T. Tadokoro, and H. Sanjoh, "50-Gb/s direct modulation of 1.3-μm InGaAlAs-based DFB laser with ridge waveguide structure," IEEE J. Sel. Top. Quantum Electron. **19**(4), 1500908 (2013).

1. Introduction

Over the past few decades, advancements in optical communication technology have enabled large-capacity transmission systems from transpacific networks to interconnect with supercomputers in data-centers [1]. Accordingly, optical communications to further short-reach applications are also being investigated. One of the ultimate challenges in this regard is on-chip optical interconnection, which has the potential to overcome the bottlenecks due to delay and Joule heating that occur in the global wiring layer of LSI chips. For such applications, optical devices are required to operate with ultra-low-power consumption [2]. In addition, a small size is needed to integrate many devices on a chip area of a few square centimeters. An effective means of achieving this is to use a strong optical confinement structure. Vertical-cavity surface-emitting lasers (VCSELs) have two high-reflection mirrors that sandwich the active layer. There are many reports on the high-speed and low-power consumption operation of VCSELs [3,4]. However, for use as the light source of an in-plane optical circuit, a mechanism to bend the output beam into the in-plane circuit is needed [5]. Various compact optical devices, such as modulators [6,7] and lasers [8], have been realized by using a microdisk cavity structure. However, the output efficiency of the structure is low

#250395 Received 22 Sep 2015; revised 22 Oct 2015; accepted 25 Oct 2015; published 29 Oct 2015

because of its evanescently coupled output waveguide. A photonic crystal laser with air-bridge structure [9] is an attractive device for an in-plane light source. Although it shows ultra-low-energy consumption operation, avalanche photodiode (APD) was used in this measurement owing to its small output power of several microwatts [10]. In general, APD requires several tens of volts and consumes more energy than a p-i-n photodiode (PD). Therefore for on-chip application, a p-i-n PD, which can operate with a reverse bias of even less than one volt, is a possible candidate. Considering that the minimum receivable power of a p-i-n PD for error free transmission is typically −13 dBm (50 μW) for 10 Gb/s signals, the required output power of the laser becomes on the order of hundreds microwatts. This means that not only low-energy consumption operation but also sufficient output power is essential. In addition to that, efficient modulation characteristics of light source is necessary. For example, to achieve 10 Gb/s operation with a bias current of 1 mA and a bias voltage of 1 V for a pulse energy cost of 100 fJ/bit [2], modulation efficiency (the slope of relaxation oscillation frequency f_r against square root of bias current above threshold) higher than 5 GHz/mA$^{1/2}$ is required since a pulse modulation speed is approximately limited by 1.3 × 1.55 f_r [11]. Moreover an increase of the modulation efficiency leads to higher modulation speed at a certain bias current. Therefore not only a reduction of the threshold current but also an increase of the modulation efficiency is required for low-power consumption operation of light sources for on-chip optical interconnections. For this purpose, an increase of modal gain by adopting a strong optical confinement structure and a reduction of operation current by adopting a small volume of active region are required.

We previously proposed and demonstrated a membrane distributed-feedback (DFB) laser as the light source of on-chip optical interconnections [12]. High-refractive index difference was obtained by using a membrane structure comprising a semiconductor core layer sandwiched by dielectric cladding layers. The optical confinement factor of the active region can be enhanced to approximately three times that of conventional double-heterostructure lasers. Furthermore, depending on the grating design, strongly index-coupled DFB lasers with an index-coupling coefficient of thousands per centimeter are attainable. These properties enable us to realize low-threshold and efficient DFB lasers. For current injection into such a dielectric cladding structure, a lateral-current-injection (LCI) structure [13,14] is a reasonable approach. Thus, the benzocyclobutene (BCB) bonding technique was used to form the membrane structure [15–19]. We consequently realized low-threshold current operation of LCI-membrane DFB laser combined with a butt-jointed built-in (BJB) waveguide [20], and its integration with p-i-n-PD [21]. Asymmetric optical output from two output waveguides was obtained by adopting a distributed-reflector (DR) structure with a power ratio between the front and rear side of 6.7 [22].

In this paper, we report on the direct modulation characteristics of membrane DFB laser bonded on a Si substrate. Under a small-signal modulation, a −3dB bandwidth of 9.5 GHz was obtained at a bias current of 1.03 mA, with a record high modulation efficiency of 9.9 GHz/mA$^{1/2}$.

2. Fabrication

The top view and cross section of the schematic device structure are shown in Figs. 1(a) and 1(b), respectively. A 270-nm-thick InP-based semiconductor layer with SiO_2 cladding layer was bonded on a Si substrate intermediated by a 2-μm-thick BCB adhesive layer. The stripe width Ws of the active region was 0.7 μm. Wet chemical etching was used to form 50-nm-deep gratings with a period of 298 nm on a 100-nm-thick InP cap layer. The DFB section (cavity length, L_{DFB} = 80 μm) was combined with the passive waveguide (length, L_{WG} = 600 μm) in order to integrate a p-i-n PD [21]. The details of initial epitaxial wafer structure and fabrication can be found in [20]. The active layers consisted of strain-compensated GaInAsP 5QWs (five 6-nm-thick 1% compressively strained quantum-wells and 10-nm-thick 0.15% tensile strained barriers) sandwiched by 15-nm-thick optical confinement layers and bottom

#250395 Received 22 Sep 2015; revised 22 Oct 2015; accepted 25 Oct 2015; published 29 Oct 2015

and top InP cap layers (50-nm and 100-nm-thick each). Selective area epitaxial growth using organometallic vapor phase epitaxy was conducted three times in order to form a passive waveguide, n-InP and p-InP regions. The wafer was bonded on a Si substrate using a BCB adhesive layer, then the InP substrate and etch stop layers were removed via polishing and wet chemical etching, respectively. The surface grating was defined using electron beam lithography. Then, the substrate was cleaved into bar form to measure the light output.

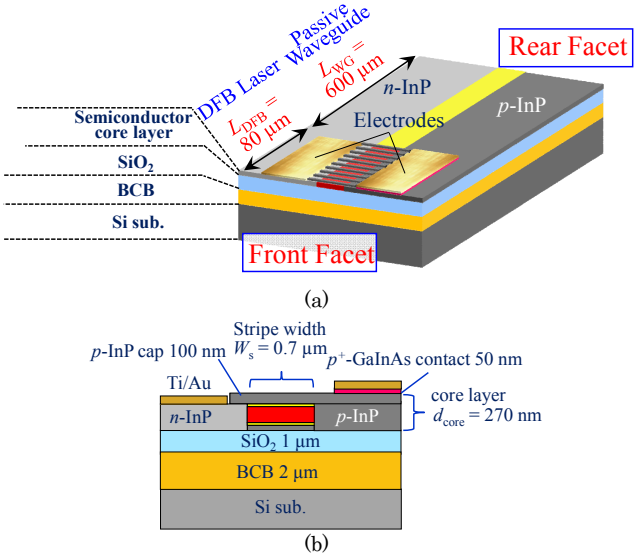

Fig. 1. Schematic structure of a membrane DFB laser: (a) top view; (b) cross section.

3. Lasing characteristics

The device was measured under room-temperature continuous-wave (RT-CW) conditions. Figure 2(a) shows light output versus injection current (*L-I*) characteristics. A low threshold operation with I_{th} = 270 μA was obtained. The threshold current density was 480 A/cm^2 (96 A/cm^2/well). The external differential quantum efficiency η_d was 12%. The maximum output power was 66 μW at an injection current of 950 μA. This is due to the leakage current through butt-jointed coupling section and large waveguide loss of our membrane stripe structure (α_{WG} = 42 cm^{-1}) [23]. When the waveguide loss is reduced to around 10 cm^{-1}, the external differential quantum efficiency from a single side will be improved to be approximately 20%. In addition to that, by introducing the DR structure that consists of both DFB and DBR sections [22,24], the differential quantum efficiency for a single side can be increased to near 40%. Hence we expect that an optical output at the same bias current can be increased to approximately 3 times higher, and it will meet the requirement for light sources for on-chip optical interconnect. Lasing spectra at two different bias currents are shown in Fig. 2(b). The lasing wavelength was 1533 nm at a bias current I_b of 410 μA (1.5I_{th}). Another lasing mode occurred when the bias current was increased to 660 μA, as depicted by the blue line. In this work as one side of the facet was formed inside the DFB section, the phase of the cleaved facet has been attributed with poor single mode property. The measured stopband width was 32 nm, which corresponds to an index-coupling coefficient of 1500 cm^{-1}. Thus, the coupling strength of cavity κL was calculated to be 12.

#250395 Received 22 Sep 2015; revised 22 Oct 2015; accepted 25 Oct 2015; published 29 Oct 2015

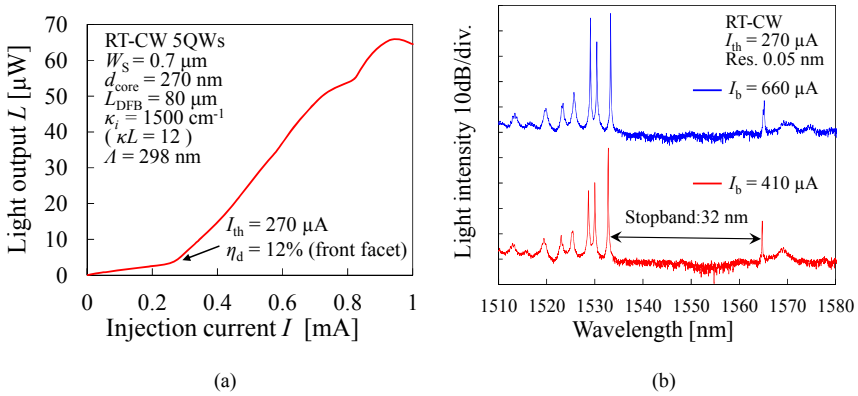

Fig. 2. Lasing characteristics of membrane DFB laser. (a) Light output versus injection current characteristics. (b) Lasing spectrum with different bias current conditions.

4. Modulation characteristics

Before performing direct modulation measurements, we measured relative intensity noise (RIN) spectrum of the membrane DFB laser. Since the peak frequency of the RIN spectrum is corresponds to the relaxation oscillation frequency f_r, we can estimate the slope efficiency of the relaxation oscillation frequency as a function of square root of the bias current above the threshold (I_b-I_{th}). Figure 3(a) shows RIN spectra for various bias currents measured at room temperature. Figure 3(b) shows the plots of relaxation oscillation frequency f_r as a function of the square root of the bias current above the threshold. From linear fitting of measured plots, the slope of the relaxation oscillation frequency of 10 GHz/mA$^{1/2}$ was obtained.

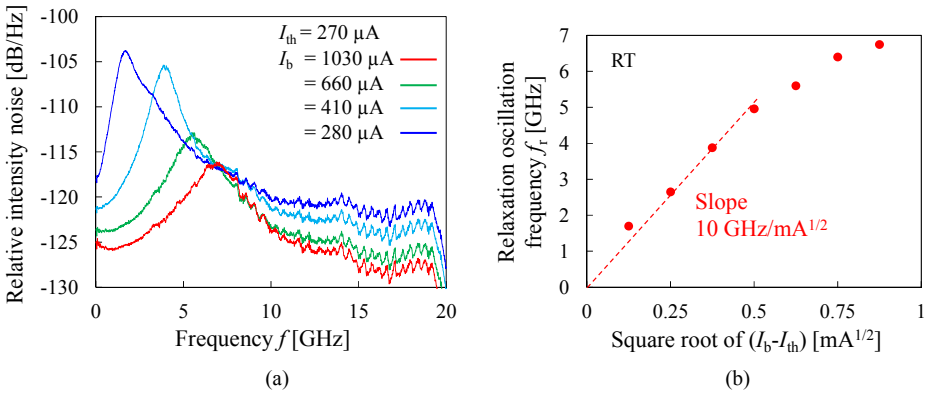

Fig. 3. Results of RIN spectrum measurements (a) RIN spectra for various bias current conditions. (b) Plots of relaxation oscillation frequency versus square root of bias current.

The small-signal frequency response of membrane DFB laser was measured using a vector network analyzer. The electrical modulation signal was directly applied to the device via a 20-GHz high-speed GS probe without impedance matching. The optical output signal from the device was collected via a spherical-lensed single-mode fiber. The coupling loss between the membrane DFB laser and lensed fiber was approximately −10 dB. The collected optical signal was amplified using an erbium-doped fiber amplifier (EDFA) to obtain optical power receivable by the photoreceiver. Then, the signal was detected by a 20-GHz bandwidth p-i-n photoreceiver. Small-signal frequency responses (S_{21}) for various bias current conditions are shown in Fig. 4. The maximum −3 dB bandwidth of 9.5 GHz was obtained at a bias

#250395 Received 22 Sep 2015; revised 22 Oct 2015; accepted 25 Oct 2015; published 29 Oct 2015

current of 1.03 mA ($3.8I_{th}$). Taking this fact into account, we can expect 10 Gb/s operation with the bias current less than 1 mA. We extracted the damping factor by fitting the results of the small-signal frequency response. The relationship between the damping factor γ and squared relaxation oscillation frequency f_r^2 is given by the following equation:

$$\gamma = K \cdot f_r^2 + \gamma_0 \tag{1}$$

where K is the K-factor and γ_0 is the damping offset. Figure 5 shows plots of damping factor versus squared relaxation oscillation frequency. The K-factor and offset γ_0 are 0.24 ns and 5.6 ns^{-1}, obtained from the slope and intercept of the linear fitting line. The maximum bandwidth is given by

$$MAXf_{-3dB} = \frac{2\sqrt{2}\pi}{K} \tag{2}$$

From this equation, the available maximum intrinsic bandwidth is calculated to be 37 GHz. As shown in Fig. 2(a), the light output was saturated at the bias current of around 1 mA, and increment of bandwidth also saturated. Namely, the bandwidth of this device was limited by light output saturation caused by thermal heating.

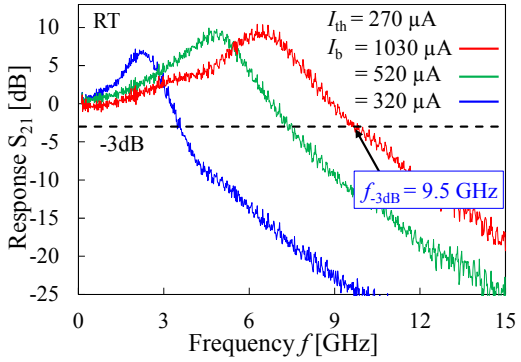

Fig. 4. Small-signal frequency response of membrane DFB laser.

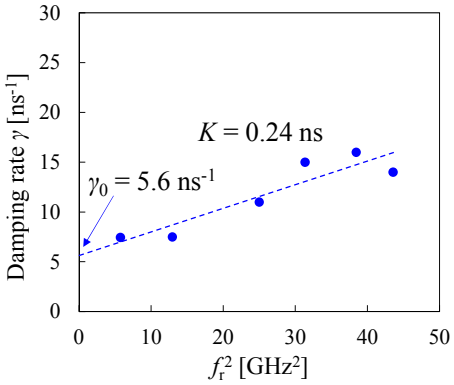

Fig. 5. Plots of damping factor versus squared relaxation oscillation frequency.

#250395 Received 22 Sep 2015; revised 22 Oct 2015; accepted 25 Oct 2015; published 29 Oct 2015

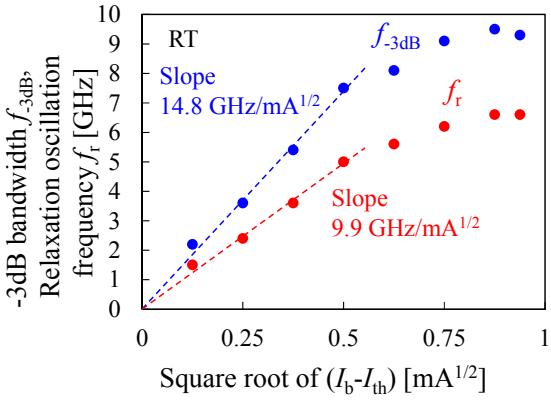

Fig. 6. Relaxation oscillation frequency and −3 dB bandwidth frequency as a function of square root of the bias current obtained from small signal frequency response.

Figure 6 shows the relaxation oscillation frequency f_r and −3 dB bandwidth f_{-3dB} as a function of the square root of the bias current. The slope of relaxation oscillation frequency and −3 dB bandwidth are 9.9 GHz/mA$^{1/2}$ and 14.8 GHz/mA$^{1/2}$, respectively. The slope of f_r well agrees with results of RIN spectrum measurements. Previously reported membrane type DFB laser showed a modulation efficiency of 7.7 GHz/mA$^{1/2}$ with a threshold current of 900 μA, and 25 Gb/s direct modulation was demonstrated [25]. Although we didn't demonstrate high-speed large-signal direct modulation, we successfully achieved lower threshold current of 270 μA and obtained the modulation efficiency of 9.9 GHz/mA$^{1/2}$, which is a record high among those of previously reported DFB lasers to the best of our knowledge. Since the active region volume V_a of our membrane DFB laser was 1.7 μm^3 (cavity length = 80 μm, stripe width = 0.7 μm, five 6-nm thick quantum wells) which was 0.65 times of that in Ref [25]. (2.6 μm^3; cavity length = 73 μm, stripe width = 1 μm, six quantum wells), we think the reason for higher modulation efficiency of our device can be attributed to the smaller volume of the active region because the modulation efficiency is proportional to inverse of square rooted active region volume $1/(V_a)^{1/2}$. By dividing the modulation efficiency of 7.7 GHz/mA$^{1/2}$ in Ref [25]. by $(0.65)^{1/2}$, the modulation efficiency of 9.6 GHz/mA$^{1/2}$ is obtained. This value well agrees with our result of 9.9 GHz/mA$^{1/2}$. We expect that the higher modulation efficiency is possible by reducing the active region volume if low threshold current density operation is maintained by strongly index-coupled structure. The modulation efficiency of conventional semiconductor cladding DFB lasers was reported to be 2.3 GHz/mA$^{1/2}$ [26] and 4.8 GHz/mA$^{1/2}$ [27] for GaInAsP-based MQW DFB laser (cavity length = 150 μm) and AlGaInAs-based MQW DFB laser (cavity length = 100 μm), respectively. Comparing with these values, our membrane DFB laser showed 2–4 times higher modulation efficiency. Since the membrane structure offers about three times higher optical confinement factor of active region than conventional laser structure [12], it leads to high modulation efficiency property of the membrane laser. The roll-off property from the linear plot occurring at $(I_b - I_{th})^{1/2} = 0.5$ mA$^{1/2}$ is due to the second lasing mode, as shown in Fig. 2(b). The decrease in the slope efficiency is caused by gain saturation. We believe that 10 G/s operation can be achieved by this membrane DFB laser with less than 1 mA bias current.

5. Conclusion

In conclusion, we performed direct modulation measurements of membrane DFB laser bonded on a Si substrate. The device exhibited a low-threshold current operation of 270 μA and an external differential quantum efficiency of 12% from the front facet. Small-signal modulation measurements indicated that a high modulation efficiency of 9.9 GHz/mA$^{1/2}$ was

#250395 Received 22 Sep 2015; revised 22 Oct 2015; accepted 25 Oct 2015; published 29 Oct 2015

obtained. These results demonstrate the benefits of using a membrane structure. Thus, membrane DFB lasers are capable of high-speed and low-power consumption operation as the light source of on-chip optical interconnection applications.

Acknowledgment

The authors would like to thank Professors S. Akiba, T. Mizumoto, M. Asada, and Y. Miyamoto, and Associate Professor M. Watanabe of the Tokyo Institute of Technology, Tokyo, Japan, for productive discussions and comments. This work was supported by JSPS KAKENHI grants, numbers 24246061, 25709026, 25420321, 15H05763, 15J04654, and 15J11776.

#250395 Received 22 Sep 2015; revised 22 Oct 2015; accepted 25 Oct 2015; published 29 Oct 2015